IEEE Access
Multidisciplinary : Rapid Review : Open Access Journal

Received 15 January 2023, accepted 6 February 2023, date of publication 16 February 2023, date of current version 9 March 2023.

Digital Object Identifier 10.1109/ACCESS.2023.3246069

RESEARCH ARTICLE

Distributed 6-DOF Coordination Control for Spacecraft Formation With Disturbance, Unmeasurable Velocity, and Communication Delays

LINTAO LI[1], YING ZHANG[1], AND RUI ZHANG[2]
[1]School of Mechanical Engineering and Automation, Harbin Institute of Technology (Shenzhen), Shenzhen, Guangdong 518055, China
[2]School of Electronic and Communication Engineering, Shenzhen Polytechnic, Shenzhen, Guangdong 518055, China

Corresponding author: Rui Zhang (zhangrui@szpt.edu.cn)

This work was supported in part by the National Natural Science Foundation of China under Grant U2013203 and Grant 62173112, in part by the Science Center Program of National Natural Science Foundation of China under Grant 62188101, and in part by the Shenzhen Science and Technology Programs under Grant RCJC20210609104400005 and Grant JCYJ20210324132413034.

ABSTRACT In this paper, the problem of distributed 6-DOF coordinated control for spacecraft formation is investigated. The dynamics of each spacecraft consisting of relative attitude and position motions are modeled into a unified Euler-Lagrange formulation. The formation consists of one virtual leader and n spacecrafts, and the information switching among the formation members is described by a directed graph. A distributed coordination control protocol is proposed to guarantee the stability of the spacecraft formation in the presence of external disturbances, unmeasurable attitude angular and position velocities, and time-varying communication delays based on the backstepping technique using time-delayed information. Further, to decrease the communication frequency of the spacecraft formation flying system, an event-triggered distributed coordination strategy is also developed to solve the 6-DOF coordinated control problem for spacecraft formation. The stability analyses of the obtained control algorithms are conducted through the Lyapunov method. Finally, the effectiveness and the ability of massive reducing the frequency of communication times of the proposed control scheme are illustrated through numerical simulations.

INDEX TERMS Spacecraft formation system, 6-DOF coordination control, communication delay, event-triggered control.

I. INTRODUCTION

In recent decades, more and more research interest has been focused on spacecraft formation flying by researchers and commercial corporations due to the fact that sending micro satellites is less-expensive. Compared with the large single spacecraft, the distributed spacecraft formation is more flexible and can share the probability of failure. Owing to these advantages, spacecraft formations have been used in different kinds of missions like meteorology observation, deep space imaging, communications, and space-laser interferometer [1], [2], [3].

There have been numerous extensive studies for spacecraft attitude control and orbit control, which are also widely extended to formation control in the existing literature. The consensus control for attitude in spacecraft formation with an undirected communication graph was investigated in [4] based on the backstepping approach, which can guarantee the fixed-time convergence of the attitude consensus errors. The attitude tracking and synchronization problem of multiple spacecraft formation with undirected communication topology and external disturbances were solved in [5] by designing a novel adaptive terminal sliding mode controller. It is proven in [5] that the proposed controller can guarantee the high accuracy of both attitude tracking and synchronization errors under external disturbance without singularity. To achieve attitude containment control for

The associate editor coordinating the review of this manuscript and approving it for publication was Engang Tian.

multiple spacecraft subjected to disturbance torques, a novel distributed adaptive finite-time controller has been developed in [6] based on the command-filtered backstepping technique. In [7], the relative position coordination tracking control for multiple spacecraft without velocity measurements has been investigated through establishing a novel filter which can estimate the velocity in finite time. Recently, more literatures trying to develop a tracking control scheme for spacecraft formation considering orbit-attitude coupling dynamics simultaneously have been available. In [8], an adaptive finite-time robust controller has been proposed to achieve the desired configuration as well as the consensus of attitudes, but this controller did not deal with the unknown velocity states. Taking physical constraints into account, the finite-time synchronization distributed control for 6-DOF dynamics with external disturbances without velocity measurements was addressed in [9], and the relative position coordination tracking control for 6-DOF dynamics with communication delays was investigated in [10] and [11]. Nevertheless, the attitude synchronization distributed control without velocity measurements and the relative position coordination tracking control has not been considered simultaneously in the existing studies. Despite advances on 6-DOF dynamics control, it is still a challenging problem on how to improve convergence speed, robustness, and stable accuracy.

In multi-agent systems, it is difficult to avoid communication delay during the process of information transmission between members. Many studies have focused on solving the communication delay problem in spacecraft formation control. Xia et al. solved the consensus problem with switching topology and communication delay in [12]. Sun and Wang [13] used the Lyapunov function method to give consensus convergence criteria for second-order systems with time-varying communication delay and dynamic topology. Wang et al. [14] proposed a finite-time convergence consensus algorithm for multi-agent system with communication delay. On the actual satellite, the available energy of communication and the bandwidth of the communication network are very limited, and the frequent communication during the control process is difficult to achieve in practice. In view of the fact that the change of the control input is very small at consecutive adjacent moments, some control methods have been proposed to reduce the frequency of control input and status information changes between neighbors based on the event-trigger strategy. The update time of the event-triggered control is determined by the trigger condition, which is the key to designing the controller. Amrr and Nabi [15] and Wu et al. [16] proposed an event-driven attitude stabilization control method for a single spacecraft, and Xu et al. [17] and Di et al. [18] proposed an attitude coordination control scheme for multiple spacecraft based on event-trigger strategy. The existing literature have not considered the communication delay between formation members and the use of event triggering strategies to reduce the communication burden between members together. In general, the researches on event-driven control of spacecraft formations are not sufficient. Designing a better trigger function for event-trigger strategy and applying it to the 6-DOF model of spacecraft formation is an open problem to be further studied.

The main contributions are summarized as follows. First, in order to estimate the unmeasurable states and disturbance, a finite-time extended state observer is developed. Then considering the unknown angular and position velocity, and the time-varying delay in the communication simultaneously, this paper addresses a 6-DOF distributed coordinated control scheme for spacecraft formation. Lastly, based on the discussions on the choice of trigger functions, a new trigger function is proposed to greatly reduce the number of triggers.

The rest of the paper is organized as follows: In Section II, the relative position and attitude of spacecraft formation are constructed, and some lemmas to be used are listed. In Section III, a distributed controller using delayed states and event-triggered strategy is driven, and the stability for the spacecraft formation system is analyzed. In Section IV, the numerical simulation is conducted and conclusions are given in Section V.

II. PRELIMINARIES

A. SPACECRAFT FORMATION ATTITUDE DYNAMICS MODEL

The modified rodrigues parameters (MRPs) is one of the commonly used descriptions of rigid body attitude motion dynamics which is simple and has no singularity problem. The MRP vector $\boldsymbol{\sigma}_i = \left[\sigma_{i1}\ \sigma_{i2}\ \sigma_{i3}\right]^{\mathrm{T}} \in \mathbb{R}^3\,(i = 1, \ldots, n)$ is defined by $\boldsymbol{\sigma}_i = \boldsymbol{e}_i \tan\frac{\phi}{4}, -2\pi < \phi < 2\pi$, where $\boldsymbol{e}_i$ represents the Euler axis unite vector and ϕ denotes the corresponding Euler rotation angle related to corresponding axis. Then the attitude kinematics and dynamics for ith spacecraft in its body-fixed frame are described by [19]

$$\begin{aligned}\dot{\boldsymbol{\sigma}}_i &= \boldsymbol{Z}(\boldsymbol{\sigma}_i)\,\boldsymbol{\omega}_i,\\ \boldsymbol{J}_i\dot{\boldsymbol{\omega}}_i &= -\boldsymbol{S}(\boldsymbol{\omega}_i)\,\boldsymbol{J}_i\boldsymbol{\omega}_i + \boldsymbol{\tau}_i + \boldsymbol{\tau}_{di},\end{aligned} \tag{1}$$

where $\boldsymbol{J}_i \in \mathbb{R}^{3\times3}$ denotes the inertia matrix of the ith spacecraft. The following expressions

$$\boldsymbol{\tau}_i = \left[\tau_{i1}\ \tau_{i2}\ \tau_{i3}\right]^{\mathrm{T}} \in \mathbb{R}^3$$

and

$$\boldsymbol{\tau}_{di} = \left[\tau_{di1}\ \tau_{di2}\ \tau_{di3}\right]^{\mathrm{T}} \in \mathbb{R}^3$$

represent the control torque and the external disturbances torque, respectively. $\boldsymbol{S}(\cdot)$ is a skew-symmetric matrix which represents the cross-product given by

$$\boldsymbol{S}(\boldsymbol{\omega}_i) = \begin{bmatrix} 0 & -\omega_i^3 & \omega_i^2 \\ \omega_i^3 & 0 & -\omega_i^1 \\ -\omega_i^2 & \omega_i^1 & 0 \end{bmatrix}$$

satisfying

$$\boldsymbol{Z}(\boldsymbol{\sigma}_i) = \frac{1}{4}[(1 - \boldsymbol{\sigma}_i^{\mathrm{T}}\boldsymbol{\sigma}_i)\boldsymbol{I}_3 + 2\boldsymbol{\sigma}_i\boldsymbol{\sigma}_i^{\mathrm{T}}] + 2\boldsymbol{S}(\sigma_i).$$

After introducing some equivalent transformation, the attitude dynamics equation of the ith spacecraft is transformed into the Euler–Lagrange form [20]

$$\boldsymbol{M}_i^{\sigma}(\boldsymbol{\sigma}_i)\ddot{\boldsymbol{\sigma}}_i + \boldsymbol{C}_i^{\sigma}(\boldsymbol{\sigma}_i,\dot{\boldsymbol{\sigma}}_i)\dot{\boldsymbol{\sigma}}_i = \boldsymbol{Z}^{-T}\boldsymbol{\tau}_i + \boldsymbol{Z}^{-T}\boldsymbol{\tau}_{di}, \quad (2)$$

where $\boldsymbol{M}_i^{\sigma}(\boldsymbol{\sigma}_i)$ and $\boldsymbol{C}_i^{\sigma}(\boldsymbol{\sigma}_i,\dot{\boldsymbol{\sigma}}_i)$ are expressed as following

$$\begin{aligned}\boldsymbol{M}_i^{\sigma}(\boldsymbol{\sigma}_i) &= \boldsymbol{Z}^{-T}\boldsymbol{J}_i\boldsymbol{Z}^{-1},\\ \boldsymbol{C}_i^{\sigma}(\boldsymbol{\sigma}_i,\dot{\boldsymbol{\sigma}}_i) &= -\boldsymbol{Z}^{-T}\boldsymbol{J}_i\boldsymbol{Z}^{-1}\dot{\boldsymbol{Z}}\boldsymbol{Z}^{-1}\\ &\quad -\boldsymbol{Z}^{-T}\boldsymbol{S}(\boldsymbol{J}_i\boldsymbol{Z}^{-1}\dot{\boldsymbol{\sigma}}_i)\boldsymbol{Z}^{-1}.\end{aligned} \quad (3)$$

It is noted that $\boldsymbol{M}_i^{\sigma}(\boldsymbol{\sigma}_i)$ is a positive definite symmetric matrix, and $\dot{\boldsymbol{M}}_i^{\sigma}(\boldsymbol{\sigma}_i) - 2\boldsymbol{C}_i^{\sigma}(\boldsymbol{\sigma}_i,\dot{\boldsymbol{\sigma}}_i)$ and $\boldsymbol{S}(\boldsymbol{J}_i\boldsymbol{Z}^{-1}(\boldsymbol{\sigma}_i)\dot{\boldsymbol{\sigma}}_i)$ are skew-symmetric matrices.

B. RELATIVE TRANSLATIONAL DYNAMICS MODEL

Assume that the virtual leader spacecraft's orbit is an ideal and elliptical orbit, and $\boldsymbol{R}_c$ denotes the distance vector between the earth geocenter and the virtual leader. Then, in the local-vertical-local-horizon (LVLH) coordinate frame attached to the leader spacecraft, $\boldsymbol{x}_c$ axis towards along the direction of $\boldsymbol{R}_c$, $\boldsymbol{z}_c$ axis points normal to the orbit plane, and $\boldsymbol{y}_c$ is mutually perpendicular to $\boldsymbol{x}_c$ and $\boldsymbol{z}_c$ such that the LVLH coordinate frame a right-handed frame. Then the relative translational dynamics model for the ith spacecraft in its LVLH frame can be obtained as [21]

$$\begin{aligned}\ddot{x}_i &= 2\dot{\theta}\dot{y}_i + \ddot{\theta}y_i + \dot{\theta}^2x_i - \frac{\mu(x_i+R_c)}{R_i^3} + \frac{\mu}{R_c^2}\\ &\quad + \frac{1}{m_i}(f_{xi}+f_{dxi}),\\ \ddot{y}_i &= -2\dot{\theta}\dot{x}_i - \ddot{\theta}x_i + \dot{\theta}^2y_i - \frac{\mu y_i}{R_i^3} + \frac{1}{m_i}(f_{yi}+f_{dyi}),\\ \ddot{z}_i &= -\frac{\mu z_i}{R_i^3} + \frac{1}{m_i}(f_{zi}+f_{dzi}),\end{aligned} \quad (4)$$

where $\boldsymbol{\rho}_i = [x_i\ y_i\ z_i]^{\mathrm{T}}$ denotes the position vector from the leader to the ith spacecraft. m_i is the mass of the ith spacecraft, R_c denotes the distance between the earth center and the leader, R_i represents the distance from the earth center to the ith spacecraft, μ is the gravitational constant, and θ is the true anomaly for the virtual leader. $\boldsymbol{f}_i = [f_{xi}\ f_{yi}\ f_{zi}]^{\mathrm{T}} \in \mathbb{R}^3$ is the control force applied on the ith spacecraft and $\boldsymbol{f}_{di} = [f_{dxi}\ f_{dyi}\ f_{dzi}]^{\mathrm{T}} \in \mathbb{R}^3$ is the external disturbance of the ith spacecraft. Then transform the relative translational dynamics model into the Euler-Lagrange form as

$$\boldsymbol{M}_i^{\rho}(\boldsymbol{\rho}_i)\ddot{\boldsymbol{\rho}}_i + \boldsymbol{C}_i^{\rho}(\boldsymbol{\rho}_i,\dot{\boldsymbol{\rho}}_i)\dot{\boldsymbol{\rho}}_i + \boldsymbol{G}_i^{\rho}(\boldsymbol{\rho}_i) = \boldsymbol{f}_i + \boldsymbol{f}_{di}, \quad (5)$$

where

$$\begin{aligned}\boldsymbol{M}_i^{\rho} &= m_i\boldsymbol{I}_3,\\ \boldsymbol{C}_i^{\rho} &= \begin{bmatrix} 0 & -2m_i\dot{\theta} & 0\\ 2\,m_i\dot{\theta} & 0 & 0\\ 0 & 0 & 0\end{bmatrix},\\ \boldsymbol{G}_i^{\rho}(\boldsymbol{\rho}_i) &= m_i\begin{bmatrix} -\ddot{\theta}y_i - \dot{\theta}^2x_i + \frac{\mu(x_i+R_c)}{R_i^3} - \frac{\mu}{R_c^2}\\ \ddot{\theta}x_i - \dot{\theta}^2y_i + \frac{\mu y_i}{R_i^3}\\ \frac{\mu z_i}{R_i^3}\end{bmatrix}.\end{aligned} \quad (6)$$

C. 6-DOF COUPLED MOTION MODEL OF SPACECRAFT FORMATION

Define $\boldsymbol{q}_i = [\boldsymbol{\sigma}_i^{\mathrm{T}}\ \boldsymbol{\rho}_i^{\mathrm{T}}]^{\mathrm{T}}$. Combining the attitude dynamics model (2) and relative translational dynamics model (5), the 6-DOF model for the ith spacecraft is presented as

$$\boldsymbol{M}_i(\boldsymbol{q}_i)\ddot{\boldsymbol{q}}_i + \boldsymbol{C}_i(\boldsymbol{q}_i,\dot{\boldsymbol{q}}_i)\dot{\boldsymbol{q}}_i + \boldsymbol{G}_i(\boldsymbol{q}_i) = \boldsymbol{H}_i\boldsymbol{u}_i + \boldsymbol{D}_i\boldsymbol{d}_i, \quad (7)$$

where

$$\begin{aligned}\boldsymbol{M}_i &= \begin{bmatrix}\boldsymbol{M}_i^{\sigma}(\boldsymbol{\sigma}_i) & 0_{3\times3}\\ 0_{3\times3} & \boldsymbol{M}_i^{\rho}\end{bmatrix},\\ \boldsymbol{C}_i &= \begin{bmatrix}\boldsymbol{C}_i^{\sigma}(\boldsymbol{\sigma}_i,\dot{\boldsymbol{\sigma}}_i) & 0_{3\times3}\\ 0_{3\times3} & \boldsymbol{C}_i^{\rho}\end{bmatrix}, \boldsymbol{G}_i = \begin{bmatrix}0_{3\times1}\\ \boldsymbol{G}_i^{\rho}(\boldsymbol{\rho}_i)\end{bmatrix},\\ \boldsymbol{u}_i &= \begin{bmatrix}\boldsymbol{\tau}_i\\ \boldsymbol{f}_i\end{bmatrix}, \boldsymbol{d}_i = \begin{bmatrix}\boldsymbol{\tau}_{di}\\ \boldsymbol{f}_{di}\end{bmatrix},\\ \boldsymbol{H}_i &= \begin{bmatrix}\boldsymbol{Z}^{-\mathrm{T}}(\boldsymbol{\sigma}_i) & 0_{3\times3}\\ 0_{3\times3} & \boldsymbol{R}_{bi}^L\end{bmatrix}, \boldsymbol{D}_i = \begin{bmatrix}\boldsymbol{Z}^{-\mathrm{T}}(\boldsymbol{\sigma}_i) & 0_{3\times3}\\ 0_{3\times3} & \boldsymbol{I}_3\end{bmatrix},\end{aligned} \quad (8)$$

where $\boldsymbol{R}_{bi}^L$ is the body-fixed frame to the LVLH frame rotation matrix.

Note that there are some properties of the 6-DOF model of spacecraft formation based on the Euler-Lagrange form. Firstly, $\boldsymbol{M}_i(\boldsymbol{q}_i)$ is a bounded symmetric positive definite matrix, thus there are two positive constants λ_1, λ_2 such that $\lambda_1\|\boldsymbol{x}\|^2 \leqslant \boldsymbol{x}^{\mathrm{T}}\boldsymbol{M}_i\boldsymbol{x} \leqslant \lambda_2\|\boldsymbol{x}\|^2$ for any $\boldsymbol{x} \in \mathbb{R}^6$. Secondly, $\dot{\boldsymbol{M}}_i(\boldsymbol{q}_i) - 2\boldsymbol{C}_i(\boldsymbol{q}_i,\dot{\boldsymbol{q}}_i)$ is a skew-symmetric matrix, which means $\boldsymbol{x}^{\mathrm{T}}(\dot{\boldsymbol{M}}_i - 2\boldsymbol{C}_i)\boldsymbol{x} = 0$ for all $\boldsymbol{x} \in \mathbb{R}^6$.

D. GRAPH THEORY

To represent the information exchanging from one spacecraft to another, the graph theory is introduced. Suppose that there are n spacecrafts in a spacecraft formation system. The communication links between the spacecraft formation are denoted by a graph $G = \{V, \varepsilon, A\}$, where each spacecraft is regarded as a node, $V = \{v_1, v_2, \ldots, v_n\}$ expresses the nodes set, and $\mathcal{A} = [a_{ij}] \in \mathbb{R}^{n\times n}$ represents the adjacency matrix. $a_{ij} = 1$ means node v_j can obtain information from node v_i and a direct edge $(v_i, v_j) \in \varepsilon$; otherwise $a_{ij} = 0$. $\mathcal{D} = \mathrm{diag}\{d_1, d_2, \ldots, d_n\}$ represents the degree matrix of the graph G, where $d_i = \sum_{j=1}^n a_{ij}$. The Laplacian matrix of the graph G can be written as $\mathcal{L} = \mathcal{D} - \mathcal{A}$, $\mathcal{L} \in \mathbb{R}^{n\times n}$.

A directed tree can be called as directed graph. There exists one root node in the directed tree owning directed paths to any other node, but there is no parent node in this directed tree. Moreover, the graph has a directed spanning tree, under the condition that in the directed graph G there is at least one root.

E. ASSUMPTIONS AND LEMMAS

Assumption 1: A spacecraft can obtain the information from another spacecraft through the directed communication topology. The communication delay from the ith spacecraft to the jth spacecraft is represented as T_{ij}, which is an unknown time-varying variable. And it is bounded by an unknown constant and its first-order derivative is assumed to satisfy $\dot{T}_{ij} < 1$.

Assumption 2: The external disturbance $\boldsymbol{d}_i$ is unknown but bounded. There exists a constant $\bar{\boldsymbol{d}} > 0$ such that $\|\boldsymbol{d}_i\| \leq \bar{\boldsymbol{d}}$.

Lemma 1: [22] The Laplacian matrix of the directed graph G is $\mathcal{L}$. If the directed graph G is strongly connected, then there exists a positive column vector $\boldsymbol{\zeta} \in \mathbb{R}^n$ such that $\boldsymbol{\zeta}^{\mathrm{T}}\mathcal{L} = \mathbf{0}$.

Lemma 2: [23] For any system $\dot{\boldsymbol{x}} = f(\boldsymbol{x}), f(0) = 0$ with $\boldsymbol{x} \in \mathbb{R}^n$, if there exists a positive definite continuous function $V(x) : U \to R$, real numbers $c > 0$ and $\alpha \in (0, 1)$, and an open neighborhood $U_0 \subset U$ near the origin, such that

$$\dot{V}(x) + cV^{\alpha}(x) \leqslant 0 \tag{9}$$

for all $\boldsymbol{x} \in U_0$, then $\boldsymbol{x}$ will converge to the origin in finite time and the converging time T satisfies

$$T \leqslant \frac{V^{1-\alpha}(x_0)}{c(1-\alpha)}. \tag{10}$$

Lemma 3: [23] For any $x_i \in \mathbb{R}$, $i = 1, 2, \ldots, n$, and real number $p \in (0, 1)$, it can be obtained

$$\sum_{i=1}^{n} \left|x_i^p\right| \geqslant \left(\sum_{i=1}^{n} |x_i|\right)^p. \tag{11}$$

III. MAIN RESULT

A. FINITE-TIME EXTENDED STATE OBSERVER

In the actual space environment, the real states of the spacecraft and the value of the lumped disturbance may not be obtained due to the restriction of the apparatus and complexity of measurements. Thus, to estimate the unmeasurable states and disturbance, the following finite-time extended state observer inspired by [24] is developed. First, denote $\boldsymbol{q}_{i1} = \boldsymbol{q}_i$, $\boldsymbol{q}_{i2} = \dot{\boldsymbol{q}}_i$. Therefore, the dynamic model (7) can be rewritten as

$$\begin{aligned} \dot{\boldsymbol{q}}_{i1} &= \boldsymbol{q}_{i2}, \\ \dot{\boldsymbol{q}}_{i2} &= \boldsymbol{M}_i^{-1}\left(\boldsymbol{H}_i\boldsymbol{u}_i + \boldsymbol{D}_i\boldsymbol{d}_i - \boldsymbol{C}_i\boldsymbol{q}_{i2} - \boldsymbol{G}_i\right). \end{aligned} \tag{12}$$

Then, the extended state observer for the ith spacecraft is designed as

$$\begin{aligned} \dot{\hat{\boldsymbol{q}}}_{i1} &= \hat{\boldsymbol{q}}_{i2} + \rho_1\left(\mathrm{sig}^{\alpha_1}(\boldsymbol{e}_{i1}) + \mathrm{sig}^{\beta_1}(\boldsymbol{e}_{i1})\right) + k_1\,\mathrm{sign}(\boldsymbol{e}_{i1}), \\ \dot{\hat{\boldsymbol{q}}}_{i2} &= \hat{\boldsymbol{q}}_{i3} + \boldsymbol{M}_i^{-1}\left(\boldsymbol{H}_i\boldsymbol{u}_i - \hat{\boldsymbol{C}}_i\hat{\boldsymbol{q}}_{i2} - \hat{\boldsymbol{G}}_i\right) \\ &\quad + \rho_2\left(\mathrm{sig}^{\alpha_2}(\boldsymbol{e}_{i1}) + \mathrm{sig}^{\beta_2}(\boldsymbol{e}_{i1})\right) + k_2\,\mathrm{sign}(\boldsymbol{e}_{i1}), \\ \dot{\hat{\boldsymbol{q}}}_{i3} &= \rho_3\left(\mathrm{sig}^{\alpha_3}(\boldsymbol{e}_{i1}) + \mathrm{sig}^{\beta_3}(\boldsymbol{e}_{i1})\right) + k_3\,\mathrm{sign}(\boldsymbol{e}_{i1}), \end{aligned} \tag{13}$$

where $\hat{\boldsymbol{q}}_{i1}$ and $\hat{\boldsymbol{q}}_{i2}$ are the estimates of $\boldsymbol{q}_{i1}$ and $\dot{\boldsymbol{q}}_i$, respectively. $\hat{\boldsymbol{q}}_{i3}$ is the estimate of $\boldsymbol{M}_i^{-1}\boldsymbol{D}_i\boldsymbol{d}_i$. $\boldsymbol{e}_{i1} = \boldsymbol{q}_i - \hat{\boldsymbol{q}}_{i1}$ denotes the estimate error, and $\frac{2}{3} < \alpha_1 < 1$, $\beta_1 = \frac{1}{\alpha_1}$, $\alpha_i = i\alpha_1 - (i-1)$, $\beta_i = \beta_1 + (i-1)(\alpha_1 - 1)$, $i = 2, 3$. $\rho_i > 1$, $k_i > 0$, $i = 1, 2, 3$.

Theorem 1: Consider the spacecraft formation 6-DOF dynamics (7), if the finite-time extended state observer is designed as (13), the estimate errors will converge to zero in finite time.

The proof of this theorem can be conducted through the theorem 1 in [24], so it is omitted here to save space.

B. CONTROLLER DESIGN

In this section, a distributed controller will be designed by considering communication delays between spacecrafts and using the backstepping technique. The tracking errors of attitudes and positions are expressed as $\tilde{\boldsymbol{q}}_i = \boldsymbol{q}_i - \boldsymbol{q}_i^d$. The $\boldsymbol{q}_{ri}$ is designed as

$$\boldsymbol{q}_{ri} = \dot{\boldsymbol{q}}_i^d - \sum_{j=1}^{n} a_{ij}\left[(\lambda + w)\,\tilde{\boldsymbol{q}}_i - \lambda\tilde{\boldsymbol{q}}_j\left(t - T_{ij}\right)\right], \tag{14}$$

where $\tilde{\boldsymbol{q}}_j\left(t - T_{ij}\right)$ denotes the states from the jth spacecraft undergoing T_{ij} time delay. Based on $\boldsymbol{q}_{ri}$, a distributed finite-time controller is proposed as the following

$$\begin{aligned} \boldsymbol{u}_i(t) = \boldsymbol{H}_i^{-1}\Big[&\boldsymbol{M}_i\Big(\dot{\boldsymbol{q}}_{ri} - \hat{\boldsymbol{q}}_{i3} - \rho_2\left(\mathrm{sig}^{\alpha_2}(\boldsymbol{e}_{i1}) + \mathrm{sig}^{\beta_2}(\boldsymbol{e}_{i1})\right) \\ &- k_2\,\mathrm{sign}(\boldsymbol{e}_{i1}) - l_i\,\mathrm{sig}^{\gamma}(\hat{\boldsymbol{q}}_{i2} - \boldsymbol{q}_{ri})\Big) + \hat{\boldsymbol{C}}_i\hat{\boldsymbol{q}}_{i2} + \hat{\boldsymbol{G}}_i\Big]. \end{aligned} \tag{15}$$

Theorem 2: Consider the spacecraft formation 6-DOF dynamics described by (7), and $\boldsymbol{q}_{ri}$ in (14). Under the distributed controller (15), each spacecraft velocity $\dot{\boldsymbol{q}}_i$ can converge to $\boldsymbol{q}_{ri}$, and the attitude and relative position $\boldsymbol{q}_i$ can achieve the desired values.

Proof: When the spacecraft velocity states $\dot{\boldsymbol{q}}_i$ converges to $\boldsymbol{q}_{ri}$, we have $\dot{\tilde{\boldsymbol{q}}}_i = \boldsymbol{q}_{ri} - \dot{\boldsymbol{q}}_i^d = -\sum_{j=1}^{n} a_{ij}\left[(\lambda + w_i)\,\tilde{\boldsymbol{q}}_i - \lambda\tilde{\boldsymbol{q}}_j\left(t - T_{ij}\right)\right]$.

Choose the following Lyapunov-Krasovskii function

$$V_1 = \frac{1}{2}\sum_{i=1}^{N}\zeta_i\tilde{\boldsymbol{q}}_i^{\mathrm{T}}\tilde{\boldsymbol{q}}_i + \frac{1}{2}\sum_{i=1}^{N}\zeta_i\sum_{j=1}^{N}a_{ij}\int_{t-T_{ij}}^{t}\tilde{\boldsymbol{q}}_j^{\mathrm{T}}(\tau)\,\tilde{\boldsymbol{q}}_j(\tau)\,\mathrm{d}\tau. \tag{16}$$

Taking the derivative of V_1 yields

$$\begin{aligned} \dot{V}_1 &= \sum_{i=1}^{N}\zeta_i\tilde{\boldsymbol{q}}_i^{\mathrm{T}}\left\{-\sum_{j=1}^{n}a_{ij}\Big[(\lambda + w)\,\tilde{\boldsymbol{q}}_i - \lambda\tilde{\boldsymbol{q}}_j\left(t - T_{ij}\right)\Big]\right\} \\ &\quad + \frac{1}{2}\sum_{i=1}^{N}\zeta_i\sum_{j=1}^{N}a_{ij}\Big[\tilde{\boldsymbol{q}}_j^{\mathrm{T}}\tilde{\boldsymbol{q}}_j - \left(1 - \dot{T}_{ij}\right) \\ &\quad \times\tilde{\boldsymbol{q}}_j^{\mathrm{T}}\left(t - T_{ij}\right)\tilde{\boldsymbol{q}}_j\left(t - T_{ij}\right)\Big] \\ &\leqslant -\sum_{i=1}^{N}\zeta_i\sum_{j=1}^{n}a_{ij}\left[(\lambda + w)\,\tilde{\boldsymbol{q}}_i^{\mathrm{T}}\tilde{\boldsymbol{q}}_i - \lambda\tilde{\boldsymbol{q}}_i^{\mathrm{T}}\tilde{\boldsymbol{q}}_j\left(t - T_{ij}\right)\right] \\ &\quad + \frac{1}{2}\sum_{i=1}^{N}\zeta_i\sum_{j=1}^{N}a_{ij}\left[\tilde{\boldsymbol{q}}_j^{\mathrm{T}}\tilde{\boldsymbol{q}}_j - \lambda\tilde{\boldsymbol{q}}_j^{\mathrm{T}}\left(t - T_{ij}\right)\tilde{\boldsymbol{q}}_j\left(t - T_{ij}\right)\right] \\ &\leqslant -\frac{1}{2}\sum_{i=1}^{N}\zeta_i\sum_{j=1}^{N}a_{ij}\lambda\|\tilde{\boldsymbol{q}}_i - \tilde{\boldsymbol{q}}_j\left(t - T_{ij}\right)\|^2 \\ &\quad - \frac{1}{2}\sum_{i=1}^{N}\zeta_i\sum_{j=1}^{N}a_{ij}\left(\tilde{\boldsymbol{q}}_i^{\mathrm{T}}\tilde{\boldsymbol{q}}_i - \tilde{\boldsymbol{q}}_j^{\mathrm{T}}\tilde{\boldsymbol{q}}_j\right) \\ &\quad - \sum_{i=1}^{N}\zeta_i\sum_{j=1}^{N}a_{ij}\left(\frac{1}{2}\lambda + w_i - \frac{1}{2}\right)\tilde{\boldsymbol{q}}_i^{\mathrm{T}}\tilde{\boldsymbol{q}}_i \end{aligned} \tag{17}$$

Denote $\boldsymbol{Q} = \left[\tilde{\boldsymbol{q}}_1^{\mathrm{T}}\tilde{\boldsymbol{q}}_1 \ldots \tilde{\boldsymbol{q}}_N^{\mathrm{T}}\tilde{\boldsymbol{q}}_N\right]^{\mathrm{T}}$, $\boldsymbol{\zeta} = \left[\zeta_1 \ldots \zeta_N\right]^{\mathrm{T}}$, therefore

$$\sum_{i=1}^{N}\zeta_i\sum_{j=1}^{N}a_{ij}\left(\tilde{\boldsymbol{q}}_i^{\mathrm{T}}\tilde{\boldsymbol{q}}_i-\tilde{\boldsymbol{q}}_j^{\mathrm{T}}\tilde{\boldsymbol{q}}_j\right)=\boldsymbol{\zeta}^{\mathrm{T}}\mathcal{L}\boldsymbol{Q}.$$

According to Lemma 1, $\boldsymbol{\zeta}^{\mathrm{T}}\mathcal{L}\boldsymbol{Q} = 0$ can be promised by properly choosing $\boldsymbol{\zeta}$. Thus,

$$\dot{V}_1 \leqslant -\frac{1}{2}\sum_{i=1}^{N}\zeta_i\sum_{j=1}^{N}a_{ij}\lambda\|\tilde{\boldsymbol{q}}_i-\tilde{\boldsymbol{q}}_j\left(t-T_{ij}\right)\|^2 - \sum_{i=1}^{N}\zeta_i\sum_{j=1}^{N}a_{ij}\left(\frac{1}{2}\lambda+w_i-\frac{1}{2}\right)\tilde{\boldsymbol{q}}_i^{\mathrm{T}}\tilde{\boldsymbol{q}}_i. \tag{18}$$

Now the following relations hold, $\frac{1}{2}\lambda + w_i > \frac{1}{2}$, $\dot{V}_1 \leqslant 0$. In addition, $\ddot{V}_1$ is bounded obviously. According to Barbalat's Lemma, one can conclude that $\lim_{t\to\infty}\dot{V}_1 = 0$, which means $-\frac{1}{2}\sum_{i=1}^{N}\zeta_i\sum_{j=1}^{N}a_{ij}\lambda\|\tilde{\boldsymbol{q}}_i-\tilde{\boldsymbol{q}}_j\left(t-T_{ij}\right)\|^2 = 0$, and $-\sum_{i=1}^{N}\zeta_i\sum_{j=1}^{N}a_{ij}\left(\frac{1}{2}\lambda+w_i-\frac{1}{2}\right)\tilde{\boldsymbol{q}}_i^{\mathrm{T}}\tilde{\boldsymbol{q}}_i = 0$. Therefore, it can be concluded that $\lim_{t\to\infty}\tilde{\boldsymbol{q}}_i = 0$ and $\lim_{t\to\infty}\tilde{\boldsymbol{q}}_i = \lim_{t\to\infty}\tilde{\boldsymbol{q}}_j\left(t-T_{ij}\right)$. Thus the desired attitudes and positions for the spacecraft formation will be achieved when the velocity state $\dot{\boldsymbol{q}}_i$ converges to the proposed $\boldsymbol{q}_{ri}$.

The next step is to design a distributed controller which can guarantee that each spacecraft achieves the designed velocity $\boldsymbol{q}_{ri}$. Define $\boldsymbol{e}_i = \hat{\boldsymbol{q}}_{i2} - \boldsymbol{q}_{ri}$ and choose the following Lyapunov candidate function V_2

$$V_2 = \sum_{i=1}^{N}\frac{1}{2}\boldsymbol{e}_i^{\mathrm{T}}\boldsymbol{e}_i. \tag{19}$$

Taking the derivative of V_2 leads to

$$\begin{aligned}\dot{V}_2 &= \sum_{i=1}^{N}\boldsymbol{e}_i^{\mathrm{T}}\dot{\boldsymbol{e}}_i = \sum_{i=1}^{N}\boldsymbol{e}_i^{\mathrm{T}}\left(\dot{\hat{\boldsymbol{q}}}_{i2}-\dot{\boldsymbol{q}}_{ri}\right)\\ &= \sum_{i=1}^{N}\boldsymbol{e}_i^{\mathrm{T}}\Big[\hat{\boldsymbol{q}}_{i3}+\boldsymbol{M}_i^{-1}\left(\boldsymbol{H}_i\boldsymbol{u}_i-\boldsymbol{C}_i\hat{\boldsymbol{q}}_{i2}-\boldsymbol{G}_i\right)\\ &\quad+\rho_2\left(\mathrm{sig}^{\alpha_2}(\boldsymbol{e}_{i1})+\mathrm{sig}^{\beta_2}(\boldsymbol{e}_{i1})\right)+k_2\,\mathrm{sign}(\boldsymbol{e}_{i1})-\dot{\boldsymbol{q}}_{ri}\Big].\end{aligned} \tag{20}$$

Substituting the controller (15) into (20) and referring to lemma 3, $\dot{V}_2$ can be simplified as

$$\begin{aligned}\dot{V}_2 &= \sum_{i=1}^{N}\boldsymbol{e}_i^{\mathrm{T}}\Big[-l_i\,\mathrm{sig}^{\gamma}(\hat{\boldsymbol{q}}_{i2}-\boldsymbol{q}_{ri})\Big]\\ &= \sum_{i=1}^{N}-l_i\boldsymbol{e}_i^{\mathrm{T}}\,\mathrm{sig}^{\gamma}(\boldsymbol{e}_i)\\ &\leqslant \sum_{i=1}^{N}-l_i\left(\boldsymbol{e}_i^{\mathrm{T}}\boldsymbol{e}_i\right)^{\frac{\gamma+1}{2}}\\ &\leqslant -l\left(\sum_{i=1}^{N}\boldsymbol{e}_i^{\mathrm{T}}\boldsymbol{e}_i\right)^{\frac{\gamma+1}{2}}\\ &= -2^{\frac{\gamma+1}{2}}lV_2^{\frac{\gamma+1}{2}}.\end{aligned} \tag{21}$$

According to Lemma 2, it can be concluded from (21) that $\boldsymbol{e}_i\ (i = 1, \ldots, N)$ will converge to the origin in finite time T_2, where $T_2 > 0$, and $\hat{\boldsymbol{q}}_{i2}$ will converge to $\boldsymbol{q}_{ri}$ in finite time T_2. As mentioned in Theorem 1, the estimation $\hat{\boldsymbol{q}}_{i2}$ will converge to $\dot{\boldsymbol{q}}_i$ in finite time T_1, where $T_1 > 0$. Therefore, the velocity state $\dot{\boldsymbol{q}}_i$ will reach the desired state $\boldsymbol{q}_{ri}$ in finite time T_3, where $T_3 = \max\{T_1, T_2\}$, and the desired attitudes and positions for the spacecraft formation can be achieved asymptotically when the velocity state $\dot{\boldsymbol{q}}_i$ converges to the proposed $\boldsymbol{q}_{ri}$. This completed the proof.

C. CONTROLLER DESIGN BASED ON EVENT-TRIGGERED STRATEGY

The distributed controller (15) is developed by using the time-delayed information from other spacecraft in the above section. Due to the existence of communication delays, the spacecraft in the formation may not obtain the states information from their neighbors timely. In this subsection, a controller which can reduce the burden of information transmission between spacecrafts and maintain good control performance will be constructed by introducing the event-triggered strategy. First, for the ith spacecraft, define an error variable $\boldsymbol{s}_i$ as

$$\boldsymbol{s}_i = \dot{\tilde{\boldsymbol{q}}}_i + \lambda\tilde{\boldsymbol{q}}_i, \tag{22}$$

where λ is a positive constant, and define the measurement error at time t as

$$\boldsymbol{e}_i(t) = \boldsymbol{s}_i\left(t_{k_i}^i\right) - \boldsymbol{s}_i(t), \quad t \in \left[t_{k_i}^i, t_{k_i+1}^i\right), \tag{23}$$

where $t_{k_i}^i$ represents the time when the k_ith event of spacecraft i is triggered. Then the condition of the time when the next event is triggered is defined as

$$t_{k_i+1}^i = \min\left\{t : t > t_{k_i}^i, f_i\left(t, \boldsymbol{e}_i(t)\right) \geqslant 0\right\}. \tag{24}$$

Next, design a trigger function as follows

$$\begin{aligned}f_i\left(t,\boldsymbol{e}_i(t)\right) &= \|\boldsymbol{e}_i(t)\| - \eta_i(t) - \frac{\alpha\sum_{j=1}^{n}a_{ij}\left\|\boldsymbol{s}_i\left(t_{k_i}^i\right)-\boldsymbol{s}_j\left(t_{k_j}^j\right)\right\|^2}{2\left\|\sum_{j=1}^{n}a_{ij}\left(\boldsymbol{s}_i\left(t_{k_i}^i\right)-\boldsymbol{s}_j\left(t_{k_j}^j\right)\right)\right\|},\\ \dot{\eta}_i(t) &= -\beta_i\eta_i(t) - \xi\left\|\boldsymbol{e}_i(t)\right\| + \xi\left(\frac{\alpha\sum_{j=1}^{n}a_{ij}\left\|\boldsymbol{s}_i\left(t_{k_i}^i\right)-\boldsymbol{s}_j\left(t_{k_j}^j\right)\right\|^2}{2\left\|\sum_{j=1}^{n}a_{ij}\left(\boldsymbol{s}_i\left(t_{k_i}^i\right)-\boldsymbol{s}_j\left(t_{k_j}^j\right)\right)\right\|}\right).\end{aligned}$$

Based on the above trigger function, a corresponding distributed coordination controller can be designed as below

$$\boldsymbol{q}_{ri}^{et}(t) = \dot{\boldsymbol{q}}_i^{d}(t) - \sum_{j=1}^{n}a_{ij}\left[(\lambda+\omega_i)\tilde{\boldsymbol{q}}_i(t) - \lambda\tilde{\boldsymbol{q}}_j\left(t_{k_j}^j\right)\right] \tag{25}$$

$$\begin{aligned}\boldsymbol{u}_i(t) = \boldsymbol{H}_i^{-1}\Big[&\boldsymbol{M}_i\Big(\dot{\boldsymbol{q}}_{ri}^{et}-\hat{\boldsymbol{q}}_{i3}-\rho_2\left(\mathrm{sig}^{\alpha_2}(\boldsymbol{e}_{i1})+\mathrm{sig}^{\beta_2}(\boldsymbol{e}_{i1})\right)\\ &-k_2\,\mathrm{sign}(\boldsymbol{e}_{i1})-l_i\,\mathrm{sig}^{\gamma}(\hat{\boldsymbol{q}}_{i2}-\boldsymbol{q}_{ri})\Big)+\hat{\boldsymbol{C}}_i\hat{\boldsymbol{q}}_{i2}+\hat{\boldsymbol{G}}_i\Big].\end{aligned} \tag{26}$$

Theorem 3: Consider the spacecraft formation 6-DOF dynamics described by (7), and $\boldsymbol{q}_{ri}^{et}$ represented in (25). Under the extended state observer (13) and the distributed controller (26), $\dot{\boldsymbol{q}}_i$ will converge to $\boldsymbol{q}_{ri}^{et}$, and the attitude and relative position $\boldsymbol{q}_i$ will achieve the desired values.

Proof: Similar to the proof of Theorem 2, when the spacecraft velocity states $\dot{\boldsymbol{q}}_i$ converge to $\boldsymbol{q}_{ri}^{et}$, we have $\dot{\tilde{\boldsymbol{q}}}_i = \boldsymbol{q}_{ri}^{et} - \dot{\boldsymbol{q}}_i^d = -\sum_{j=1}^{n} a_{ij}\left[(\lambda + w_i)\,\tilde{\boldsymbol{q}}_i - \lambda\tilde{\boldsymbol{q}}_j\left(t_{k_j}^j\right)\right]$. Choose the following Lyapunov-Krasovskii function

$$V_1 = \frac{1}{2}\sum_{i=1}^{N}\zeta_i\tilde{\boldsymbol{q}}_i^{\mathrm{T}}\tilde{\boldsymbol{q}}_i + \frac{1}{2}\sum_{i=1}^{N}\zeta_i\sum_{j=1}^{N}a_{ij}\int_{t_{k_j}^j}^{t}\tilde{\boldsymbol{q}}_j^{\mathrm{T}}(\tau)\,\tilde{\boldsymbol{q}}_j(\tau)\,\mathrm{d}\tau. \tag{27}$$

Taking the derivative of V_1, we have

$$\begin{aligned}
\dot{V}_1 &= \sum_{i=1}^{N}\zeta_i\tilde{\boldsymbol{q}}_i^{\mathrm{T}}\dot{\tilde{\boldsymbol{q}}}_i \\
&\quad + \frac{1}{2}\sum_{i=1}^{N}\zeta_i\sum_{j=1}^{N}a_{ij}\left[\tilde{\boldsymbol{q}}_j^{\mathrm{T}}\tilde{\boldsymbol{q}}_j - \left(1 - \dot{T}_{ij}\right)\tilde{\boldsymbol{q}}_j^{\mathrm{T}}\left(t_{k_j}^j\right)\tilde{\boldsymbol{q}}_j\left(t_{k_j}^j\right)\right] \\
&\leqslant -\frac{1}{2}\sum_{i=1}^{N}\zeta_i\sum_{j=1}^{N}a_{ij}\lambda\|\tilde{\boldsymbol{q}}_i - \tilde{\boldsymbol{q}}_j\left(t_{k_j}^j\right)\|^2 \\
&\quad -\frac{1}{2}\sum_{i=1}^{N}\zeta_i\sum_{j=1}^{N}a_{ij}\left(\tilde{\boldsymbol{q}}_i^{\mathrm{T}}\tilde{\boldsymbol{q}}_i - \tilde{\boldsymbol{q}}_j^{\mathrm{T}}\tilde{\boldsymbol{q}}_j\right) \\
&\quad -\sum_{i=1}^{N}\zeta_i\sum_{j=1}^{N}a_{ij}\left(\frac{1}{2}\lambda + \omega_i - \frac{1}{2}\right)\tilde{\boldsymbol{q}}_i^{\mathrm{T}}\tilde{\boldsymbol{q}}_i.
\end{aligned} \tag{28}$$

Similarly, define $\boldsymbol{Q} = \left[\tilde{\boldsymbol{q}}_1^{\mathrm{T}}\tilde{\boldsymbol{q}}_1 \ \ldots \ \tilde{\boldsymbol{q}}_N^{\mathrm{T}}\tilde{\boldsymbol{q}}_N\right]^{\mathrm{T}}$, $\boldsymbol{\zeta} = \left[\zeta_1 \ \ldots \ \zeta_N\right]^{\mathrm{T}}$, then one can obtain

$$\sum_{i=1}^{N}\zeta_i\sum_{j=1}^{N}a_{ij}\left(\tilde{\boldsymbol{q}}_i^{\mathrm{T}}\tilde{\boldsymbol{q}}_i - \tilde{\boldsymbol{q}}_j^{\mathrm{T}}\tilde{\boldsymbol{q}}_j\right) = \boldsymbol{\zeta}^{\mathrm{T}}\mathcal{L}\boldsymbol{Q}. \tag{29}$$

According to Lemma 1, we can ensure $\boldsymbol{\zeta}^{\mathrm{T}}\mathcal{L}\boldsymbol{Q} = 0$ by properly choosing $\boldsymbol{\zeta}$. Further, (28) can be simplified to

$$\begin{aligned}
\dot{V}_1 &\leqslant -\frac{1}{2}\sum_{i=1}^{N}\zeta_i\sum_{j=1}^{N}a_{ij}\lambda\|\tilde{\boldsymbol{q}}_i - \tilde{\boldsymbol{q}}_j\left(t_{k_j}^j\right)\|^2 \\
&\quad -\sum_{i=1}^{N}\zeta_i\sum_{j=1}^{N}a_{ij}\left(\frac{1}{2}\lambda + \omega_i - \frac{1}{2}\right)\tilde{\boldsymbol{q}}_i^{\mathrm{T}}\tilde{\boldsymbol{q}}_i
\end{aligned} \tag{30}$$

where $\frac{1}{2}\lambda + w_i > \frac{1}{2}$, so $\dot{V}_1 \leqslant 0$. In addition, $\ddot{V}_1$ is bounded obviously. According to Barbalat's Lemma, we can conclude that $\lim_{t\to\infty}\dot{V}_1 = 0$, which means $-\frac{1}{2}\sum_{i=1}^{N}\zeta_i\sum_{j=1}^{N}a_{ij}\lambda\|\tilde{\boldsymbol{q}}_i - \tilde{\boldsymbol{q}}_j\left(t_{k_j}^j\right)\|^2 = 0$, and $-\sum_{i=1}^{N}\zeta_i\sum_{j=1}^{N}a_{ij}\left(\frac{1}{2}\lambda + w_i - \frac{1}{2}\right)\tilde{\boldsymbol{q}}_i^{\mathrm{T}}\tilde{\boldsymbol{q}}_i = 0$. Therefore, we can obtain $\lim_{t\to\infty}\tilde{\boldsymbol{q}}_i = 0$ and $\lim_{t\to\infty}\tilde{\boldsymbol{q}}_i = \lim_{t\to\infty}\tilde{\boldsymbol{q}}_j\left(t_{k_j}^j\right)$. Thus the desired attitudes and positions for the spacecraft formation will be achieved when the velocity state $\dot{\boldsymbol{q}}_i$ converges to the proposed $\boldsymbol{q}_{ri}^{et}$. The rest of the proof idea is similar to Theorem 2, thus is omitted here.

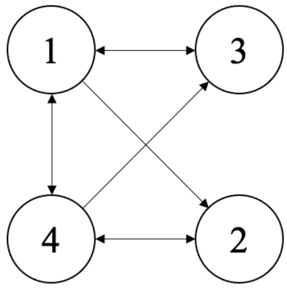

FIGURE 1. Communication topology.

IV. NUMERICAL SIMULATIONS

Consider a spacecraft formation with four following spacecrafts and a virtual spacecraft as the leader. The virtual leader is assumed to be on an elliptical orbit with the semi-major axis $a = 6621$km, right ascension of the ascending node is 60°, inclination $i = 60°$, and true anomaly $\theta = 0°$. The mass of the spacecraft is assumed to be $m_1 = m_2 = m_3 = m_4 = 10$kg and the inertia matrices of the spacecraft are set as

$$\boldsymbol{J}_1 = \boldsymbol{J}_2 = \boldsymbol{J}_3 = \boldsymbol{J}_4 = \begin{bmatrix} 5.06 & 1 & 0.5 \\ 1 & 5.07 & 1.2 \\ 0.5 & 1.2 & 5.95 \end{bmatrix}\mathrm{kg}\cdot\mathrm{m}^2. \tag{31}$$

The initial states, the desired attitudes and positions and the disturbance for each spacecraft are given in Table 1.

Consider time delays when each spacecraft receives messages from its neighbors. Assume the time delays between spacecrafts are equal and their derivatives are less than 1. Specifically, the time delays between spacecraft 1 and spacecraft 2 are set as $T_{12} = T_{21} = 1 + 0.2\sin 0.01t$ seconds, the time delays between spacecraft 1 and spacecraft 3 are set as $T_{13} = T_{31} = 1 + 0.2\cos 0.01t$ seconds, the time delays between spacecraft 1 and spacecraft 4 are set as $T_{14} = T_{41} = 1 - 0.2\sin 0.02t$ seconds, the time delays between spacecraft 2 and spacecraft 3 are set as $T_{23} = T_{32} = 1 - 0.2\cos 0.02t$ seconds, the time delays between spacecraft 2 and spacecraft 4 are set as $T_{24} = T_{42} = 1 + 0.2\,|\sin 0.02t|$ seconds, the time delays between spacecraft 3 and spacecraft 4 are set as $T_{34} = T_{43} = 1 - 0.2\,|\cos 0.02t|$ seconds. Parameters in the extended state observer (13) are chosen as $\rho_1 = \rho_2 = \rho_3 = 7$, $k_1 = k_2 = k_3 = 0.1$, $\alpha_1 = \frac{7}{9}$, $\beta_1 = \frac{9}{7}$, $\alpha_2 = \frac{5}{9}$, $\beta_2 = \frac{67}{63}$, $\alpha_3 = \frac{1}{3}$, $\beta_3 = \frac{53}{63}$. The parameters in $\boldsymbol{q}_{ri}$ are set as $\lambda = 0.6$ and $w = 0.6$, and parameters in the controller (15) are set as $l_i = 1, \gamma = \frac{1}{2}$. The communication topology of the spacecraft formation is depicted in Fig. 1 and the adjacency matrix can be attained as

$$\boldsymbol{A} = \begin{bmatrix} 0 & 0 & 1 & 1 \\ 1 & 0 & 0 & 1 \\ 1 & 0 & 0 & 1 \\ 1 & 1 & 0 & 0 \end{bmatrix}. \tag{32}$$

The simulation results are illustrated in Fig. 2-Fig. 5. Fig. 2-Fig. 3 show the attitude and relative position tracking errors of four spacecrafts, from which we can see that the following spacecraft can track the desired attitudes and positions in finite time. It can be observed from Fig. 2 that the attitudes of all four following spacecrafts are synchronized

TABLE 1. **Initial states, desired states and disturbance.**

States	Values
Initial attitudes	$\boldsymbol{\sigma}_1 = [0.1, -0.1, 0.2]^{\mathrm{T}} \quad \boldsymbol{\sigma}_2 = [0.2, -0.8, 0.4]^{\mathrm{T}}$
	$\boldsymbol{\sigma}_3 = [-0.5, -0.4, 0.7]^{\mathrm{T}} \quad \boldsymbol{\sigma}_4 = [0.1, -0.6, 0.7]^{\mathrm{T}}$
	$\dot{\boldsymbol{\sigma}}_1 = \dot{\boldsymbol{\sigma}}_2 = \dot{\boldsymbol{\sigma}}_3 = \dot{\boldsymbol{\sigma}}_4 = [0, 0, 0]^{\mathrm{T}}$
Initial positions (m)	$\boldsymbol{\rho}_1 = [25, -10, 43]^{\mathrm{T}} \quad \boldsymbol{\rho}_2 = [-5, -39, 13]^{\mathrm{T}}$
	$\boldsymbol{\rho}_3 = [29, 37, -23]^{\mathrm{T}} \quad \boldsymbol{\rho}_4 = [-19.2, 31, -56]^{\mathrm{T}}$
	$\dot{\boldsymbol{\rho}}_1 = \dot{\boldsymbol{\rho}}_2 = \dot{\boldsymbol{\rho}}_3 = \dot{\boldsymbol{\rho}}_4 = [0, 0, 0]^{\mathrm{T}}$
Desired attitudes	$\boldsymbol{\sigma}_1^{\mathrm{d}} = \boldsymbol{\sigma}_2^{\mathrm{d}} = \boldsymbol{\sigma}_3^{\mathrm{d}} = \boldsymbol{\sigma}_4^{\mathrm{d}} = [0.006 \sin(0.1t), 0.007 \cos(0.1t), 0.008 \cos(0.1t)]^{\mathrm{T}}$
Desired positions(m)	$\boldsymbol{\rho}_1^{\mathrm{d}} = \left[-5 \cos(\frac{3\pi}{T} t), 10 \sin(\frac{3\pi}{T} t), -5\sqrt{3} \cos(\frac{3\pi}{T} t)\right]^{\mathrm{T}}$
	$\boldsymbol{\rho}_2^{\mathrm{d}} = \left[-5 \cos(\frac{3\pi}{T} t + \frac{\pi}{2}), 10 \sin(\frac{3\pi}{T} t + \frac{\pi}{2}), -5\sqrt{3} \cos(\frac{3\pi}{T} t + \frac{\pi}{2})\right]^{\mathrm{T}}$
	$\boldsymbol{\rho}_3^{\mathrm{d}} = \left[-5 \cos(\frac{3\pi}{T} t + \pi), 10 \sin(\frac{3\pi}{T} t + \pi), -5\sqrt{3} \cos(\frac{3\pi}{T} t + \pi)\right]^{\mathrm{T}}$
	$\boldsymbol{\rho}_4^{\mathrm{d}} = \left[-5 \cos(\frac{3\pi}{T} t + \frac{3}{2}\pi), 10 \sin(\frac{3\pi}{T} t + \frac{3}{2}\pi), -5\sqrt{3} \cos(\frac{3\pi}{T} t + \frac{3}{2}\pi)\right]^{\mathrm{T}}$
Disturbance	$\boldsymbol{d}_1 = -1.5 \times 10^{-3} [\cos(0.1t), \sin(0.1t), 1, \cos(0.03t), 2 \sin(0.05t), -\cos(0.04t)]^{\mathrm{T}}$
	$\boldsymbol{d}_2 = 0.5 \times 10^{-3} [\sin(0.2t), 1, \cos(0.1t), -\cos(0.07t), 1.5 \sin(0.05t), \sin(0.04t)]^{\mathrm{T}}$
	$\boldsymbol{d}_3 = -0.5 \times 10^{-3} [\cos(0.1t), \cos(0.2t), 1, \cos(0.03t), 2 \cos(0.05t), \sin(0.04t)]^{\mathrm{T}}$
	$\boldsymbol{d}_4 = 1.5 \times 10^{-3} [\cos(0.2t), \sin(0.1t), 1, \sin(0.07t), \cos(0.05t), -2 \sin(0.04t)]^{\mathrm{T}}$

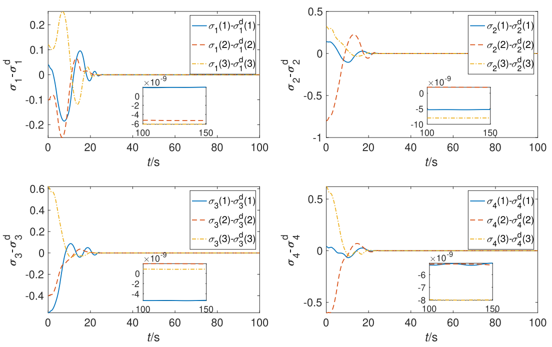

FIGURE 2. **Attitude tracking errors under observer (13) and controller (15).**

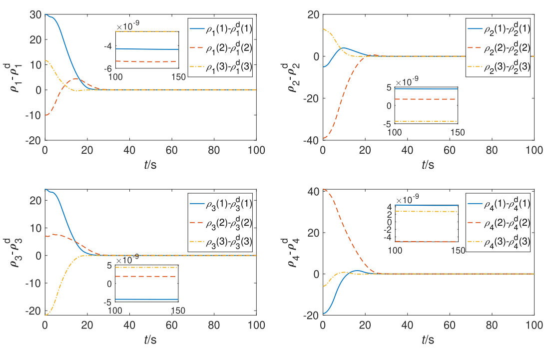

FIGURE 3. **Relative position tracking errors under observer (13) and controller (15).**

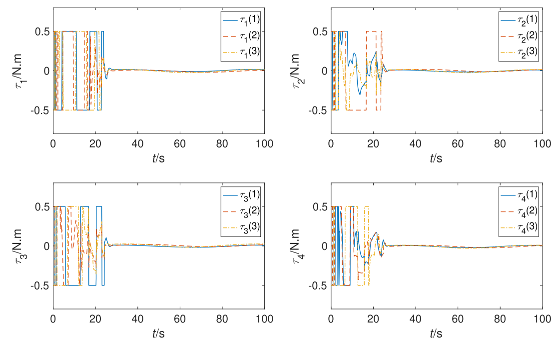

FIGURE 4. **Control torques under observer (13) and controller (15).**

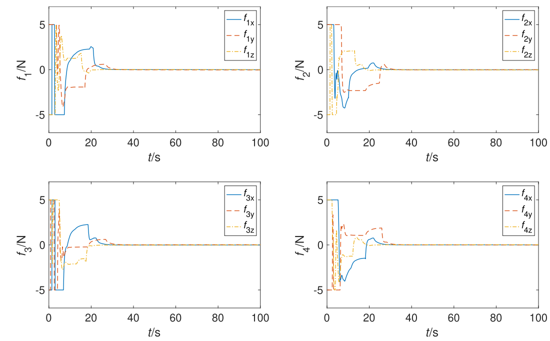

FIGURE 5. **Control forces under observer (13) and controller (15).**

to the desirable attitudes after about 25 seconds, and the attitude tracking errors can converge to regions $|\sigma_j(i) - \sigma_j^{\mathrm{d}}(i)| \leq 10^{-9}$, $(i = 1, 2, 3,\ j = 1, 2, 3, 4)$. As shown in Fig. 3, the four spacecrafts can reach the desired formation configuration after about 30 seconds, and the relative position tracking errors can converge to regions $|\rho_j(i) - \rho_j^{\mathrm{d}}(i)| \leq 2 \times 10^{-9}$, $(i = 1, 2, 3,\ j = 1, 2, 3, 4)$. The control torques and control forces of each spacecraft are depicted in Fig. 4-Fig. 5. With the desired relative position and attitude synchronization reached, the 6-DOF coordination control of spacecraft formation is achieved.

Next, consider 6-DOF coordination control for spacecraft formation under the proposed event-triggered controller (26). The simulation results are shown in Fig. 6-9. It can be observed from Fig. 6 that the attitudes of all four following spacecrafts are synchronized to the desired attitudes after about 40 seconds, and the attitude tracking errors can converge to regions $|\sigma_j(i) - \sigma_j^{\mathrm{d}}(i)| \leq 5 \times 10^{-5}$, $(i = 1, 2, 3,\ j = 1, 2, 3, 4)$ after 100 seconds. As shown in Fig. 7, the four spacecrafts can reach the desired formation configuration after about 40 seconds, and the relative position tracking errors can converge to regions $|\rho_j(i) - \rho_j^{\mathrm{d}}(i)| \leq 2 \times 10^{-5}$, $(i = 1, 2, 3,\ j = 1, 2, 3, 4)$ after 100 seconds. The control

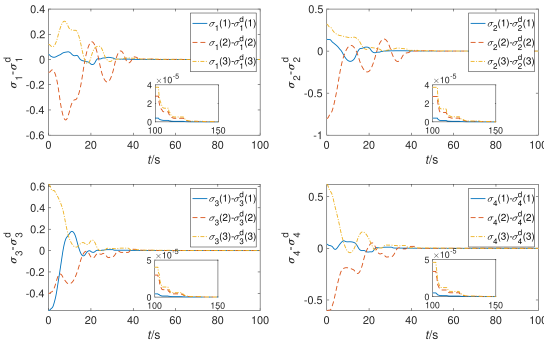

FIGURE 6. Attitudes tracking errors under observer (13) and controller (26).

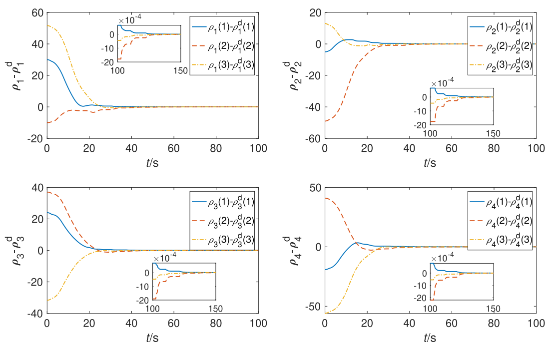

FIGURE 7. Relative positions tracking errors under observer (13) and controller (26).

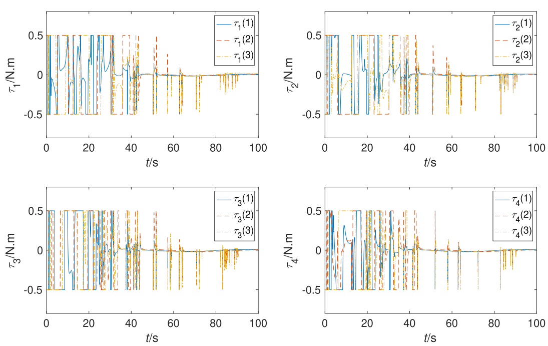

FIGURE 8. Control torques under observer (13) and controller (26).

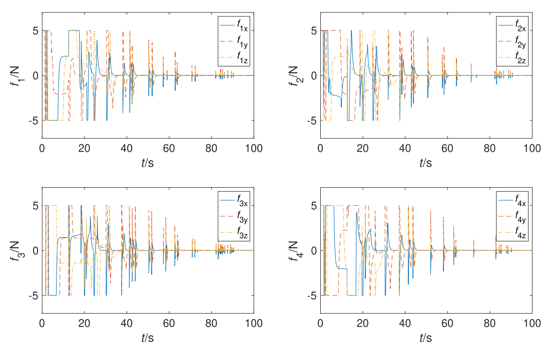

FIGURE 9. Control forces under observer (13) and controller (26).

torques and control forces of each spacecraft are depicted in Fig. 8-Fig. 9. From the simulation results, the control output encounter changes at the time when the trigger function is triggered. Compared with the established controller (15), the proposed event-triggered controller (26) can greatly reduce

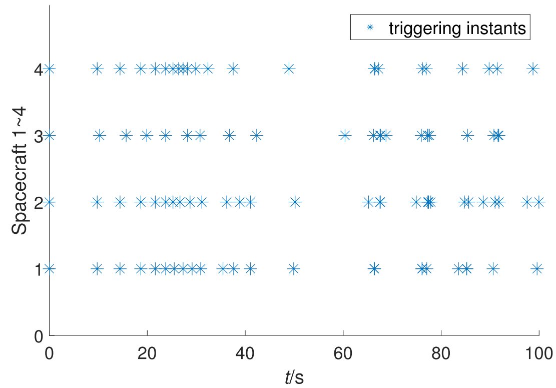

FIGURE 10. Trigger time of four spacecraft in [25].

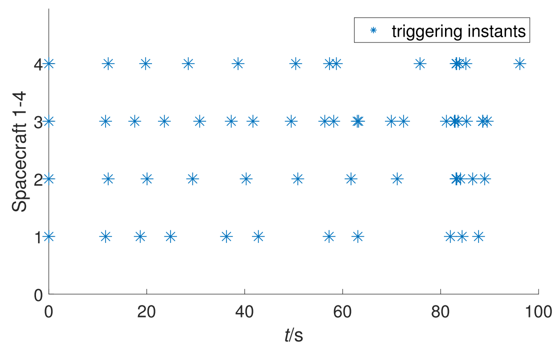

FIGURE 11. Trigger time of four spacecraft in Theorem 3.

the number of communications between spacecrafts and the communication loss of spacecraft formation. Besides, consider the following trigger function in [25],

$$f_i\left(t, \boldsymbol{e}_i(t)\right) = \|\boldsymbol{e}_i(t)\| - ae^{-bt} - \frac{\alpha \sum_{j=1}^{n} a_{ij} \left\| \boldsymbol{s}_i\left(t_{k_i}^i\right) - \boldsymbol{s}_j\left(t_{k_j}^j\right) \right\|^2}{2\left\| \sum_{j=1}^{n} a_{ij} \left(\boldsymbol{s}_i\left(t_{k_i}^i\right) - \boldsymbol{s}_j\left(t_{k_j}^j\right)\right) \right\|}.$$

The trigger times of the event-triggered controller in [25] and the proposed event-triggered controller (26) are illustrated in Fig. 10 and Fig. 11, respectively. Compared with these two event-triggered controllers under the premise of the same control accuracy, the number of triggers has been reduced by nearly 50% under the proposed event-triggered controller (26), which greatly saves the limited resources and bandwidths carried on spacecraft.

V. CONCLUSION

The distributed relative attitude and position coupling control for spacecraft formation considering communication delays is addressed in this paper. The briefer Euler-Lagrange form equation is employed to describe the 6-DOF spacecraft formation motion. The directed graph is introduced to express the information exchanging between spacecrafts. Two distributed coordination control protocols are developed based on the backstepping technique, which can guarantee the spacecraft formation to the desired configuration and consensus of attitudes in the presence of communication delays and unmeasurable velocity. The asymptotic stability of the 6-DOF spacecraft formation system is proved by selecting a suitable Lyapunov-Krasovskii function. Finally, the effectiveness of the control law is verified through simulations and the comparison with the event-triggered controller in [25] shows the proposed event-triggered method can largely reduce the frequency of communication under the premise of the same control accuracy. Our further studies will be concentrated on finite-time control for spacecraft formation with communication delays.

REFERENCES

[1] M. G. Di, M. Lawn, and R. Bevilacqua, "Survey on guidance navigation and control requirements for spacecraft formation-flying missions," *J. Guid. Control Dyn.*, vol. 41, no. 3, pp. 581–602, 2018.

[2] A.-M. Zou, A. H. J. de Ruite, and K. D. Kumar, "Distributed finite-time velocity-free attitude coordination control for spacecraft formations," *Automatica*, vol. 67, pp. 46–53, May 2016.

[3] G.-P. Liu and S. Zhang, "A survey on formation control of small satellites," *Proc. IEEE*, vol. 106, no. 3, pp. 440–457, Mar. 2018.

[4] A. Zou and Z. Fan, "Distributed fixed-time attitude coordination control for multiple rigid spacecraft," *Int. J. Robust Nonlinear Control*, vol. 30, no. 1, pp. 266–281, Jan. 2020.

[5] C. Zhang, J. Wang, D. Zhang, and X. Shao, "Synchronization and tracking of multi-spacecraft formation attitude control using adaptive sliding mode," *Asian J. Control*, vol. 21, no. 2, pp. 832–846, Mar. 2019.

[6] L. Zhao, J. Yu, and P. Shi, "Command filtered backstepping-based attitude containment control for spacecraft formation," *IEEE Trans. Syst., Man, Cybern., Syst.*, vol. 51, no. 2, pp. 1278–1287, Feb. 2021.

[7] Q. Hu and J. Zhang, "Relative position finite-time coordinated tracking control of spacecraft formation without velocity measurements," *ISA Trans.*, vol. 54, pp. 60–74, Jan. 2015.

[8] J. Zhang, D. Ye, J. D. Biggs, and Z. Sun, "Finite-time relative orbit-attitude tracking control for multi-spacecraft with collision avoidance and changing network topologies," *Adv. Space Res.*, vol. 63, no. 3, pp. 1161–1175, Feb. 2019.

[9] Y. Huang and Y. Jia, "Adaptive finite time distributed 6-DOF synchronization control for spacecraft formation without velocity measurement," *Nonlinear Dyn.*, vol. 95, no. 3, pp. 2275–2291, Feb. 2019.

[10] D. Ran, X. Chen, A. K. Misra, and B. Xiao, "Relative position coordinated control for spacecraft formation flying with communication delays," *Acta Astronaut.*, vol. 137, pp. 302–311, Aug. 2017.

[11] P. Li, Z. Liu, C. He, Q. Liu, and X.-Q. Liu, "Distributed adaptive fault-tolerant control for spacecraft formation with communication delays," *IEEE Access*, vol. 8, pp. 118653–118663, 2020.

[12] H. Xia, T.-Z. Huang, J.-L. Shao, and J.-Y. Yu, "Group consensus of multi-agent systems with communication delays," *Neurocomputing*, vol. 171, pp. 1666–1673, Aug. 2016.

[13] Y. Sun and L. Wang, "Consensus problems in networks of agents with double-integrator dynamics and time-varying delays," *Int. J. Control*, vol. 82, no. 10, pp. 1937–1945, Aug. 2009.

[14] L. Wang, Z. Chen, Z. Liu, and Z. Yuan, "Finite time agreement protocol design of multi-agent systems with communication delays," *Asian J. Control*, vol. 11, no. 3, pp. 281–286, May 2009.

[15] S. M. Amrr and M. Nabi, "Attitude stabilization of flexible spacecraft under limited communication with reinforced robustness," *Trans. Inst. Meas. Control*, vol. 41, no. 16, pp. 4475–4487, Dec. 2019.

[16] B. Wu, Q. Shen, and X. Cao, "Event-triggered attitude control of spacecraft," *Adv. Space Res.*, vol. 61, no. 3, pp. 927–934, 2018.

[17] C. Xu, B. Wu, X. Cao, and Y. Zhang, "Distributed adaptive event-triggered control for attitude synchronization of multiple spacecraft," *Nonlinear Dyn.*, vol. 95, no. 4, pp. 2625–2638, Mar. 2019.

[18] F.-Q. Di, A.-J. Li, Y. Guo, C.-Q. Xie, and C.-Q. Wang, "Event-triggered sliding mode attitude coordinated control for spacecraft formation flying system with disturbances," *Acta Astronaut.*, vol. 188, pp. 121–129, Nov. 2021.

[19] L. Zhao and Y. Jia, "Decentralized adaptive attitude synchronization control for spacecraft formation using nonsingular fast terminal sliding mode," *Nonlinear Dyn.*, vol. 78, no. 4, pp. 2779–2794, Dec. 2014.

[20] Z. Meng, W. Ren, and Z. You, "Distributed finite-time attitude containment control for multiple rigid bodies," *Automatica*, vol. 46, no. 12, pp. 2092–2099, 2010.

[21] D. Ran, X. Chen, and A. K. Misra, "Finite time coordinated formation control for spacecraft formation flying under directed communication topology," *Acta Astronaut.*, vol. 136, pp. 125–136, Jul. 2017.

[22] F. Xiao, J. Chen, and L. Wang, "Finite-time formation control for multi-agent systems," *Automatica*, vol. 45, no. 11, pp. 2605–2611, 2009.

[23] H. Du, S. Li, and C. Qian, "Finite-time attitude tracking control of spacecraft with application to attitude synchronization," *IEEE Trans. Autom. Control*, vol. 56, no. 11, pp. 2711–2717, Nov. 2011.

[24] S. Xiong, W. Wang, X. Liu, Z. Chen, and S. Wang, "A novel extended state observer," *ISA Trans.*, vol. 58, pp. 309–317, Sep. 2015.

[25] Q. Liu, M. Ye, J. Qin, and C. Yu, "Event-triggered algorithms for leader–follower consensus of networked Euler–Lagrange agents," *IEEE Trans. Syst., Man, Cybern., Syst.*, vol. 49, no. 7, pp. 1435–1447, Jul. 2019.

LINTAO LI was born in Sichuan. He received the B.Eng. degree in detection, guidance and control engineering from the Nanjing University of Aeronautics and Astronautics, in 2019, and the M.Eng. degree in control engineering from the Harbin Institute of Technology, Shenzhen, in 2022. His main research interests include multi-agent control and distributed control of spacecraft formation.

YING ZHANG was born in Jilin. She received the M.Eng. degree in control theory and control engineering from the Harbin University of Science and Technology, in 2003, and the Ph.D. degree in control science and engineering from the Harbin Institute of Technology, Shenzhen, in 2007. From 2007 to 2010, she was a Postdoctoral Researcher at the Shenzhen Graduate School, Harbin Institute of Technology, where she became an Assistant Professor, in 2010, and an Associate Professor, in 2011. She is currently an Associate Professor with the Harbin Institute of Technology. Her main research interests include spacecraft control, robust control, and filter theory.

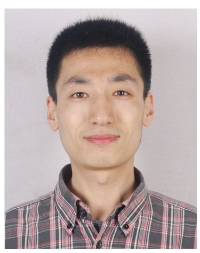

RUI ZHANG was born in Heilongjiang. He received the M.Eng. degree in control theory and control engineering from the Harbin University of Science and Technology, in 2003, and the Ph.D. degree in control science and engineering from the Harbin Institute of Technology, in 2008. From 2008 to 2014, he was a Research Assistant at the Shenzhen Institute of Advanced Technology, Chinese Academy of Sciences. From 2014 to 2015, he visited at the Department of Electrical, Electronic, and Computer Engineering, University of Western Australia, Australia. Since 2016, he has been with the School of Electronic and Communication Engineering, Shenzhen Polytechnic. His current interests include spacecraft control and robust control.